AIP | Journal of Applied Physics

Photoluminescence decay rate engineering of CdSe quantum dots in ensemble arrays embedded with gold nano-antennae

M. Haridas, J. K. Basu, A. K. Tiwari, and M. Venkatapathi

Citation: J. Appl. Phys. **114**, 064305 (2013); doi: 10.1063/1.4817650
View online: http://dx.doi.org/10.1063/1.4817650
View Table of Contents: http://jap.aip.org/resource/1/JAPIAU/v114/i6
Published by the AIP Publishing LLC.

JOURNAL OF APPLIED PHYSICS **114**, 064305 (2013)

Photoluminescence decay rate engineering of CdSe quantum dots in ensemble arrays embedded with gold nano-antennae

M. Haridas,[1] J. K. Basu,[1,a)] A. K. Tiwari,[2] and M. Venkatapathi[2]
[1]*Department of Physics, Indian Institute of Science, Bangalore 560012, India*
[2]*Computational Photonics Laboratory, SERC, Indian Institute of Science, Bangalore 560012, India*

(Received 11 June 2013; accepted 22 July 2013; published online 9 August 2013)

We discuss experimental results on the ability to significantly tune the photoluminescence decay rates of CdSe quantum dots embedded in an ordered template, using lightly doped small gold nanoparticles (nano-antennae), of relatively low optical efficiency. We observe both enhancement and quenching of photoluminescence intensity of the quantum dots varying monotonically with increasing volume fraction of added gold nanoparticles, with respect to undoped quantum dot arrays. However, the corresponding variation in lifetime of photoluminescence spectra decay shows a hitherto unobserved, non-monotonic variation with gold nanoparticle doping. We also demonstrate that Purcell effect is quite effective for the larger (5 nm) gold nano-antenna leading to more than four times enhanced radiative rate at spectral resonance, for largest doping and about 1.75 times enhancement for off-resonance. Significantly for spectral off-resonance samples, we could simultaneously engineer reduction of non-radiative decay rate along with increase of radiative decay rate. Non-radiative decay dominates the system for the smaller (2 nm) gold nano-antenna setting the limit on how small these plasmonic nano-antennae could be to be effective in engineering significant enhancement in radiative decay rate and, hence, the overall quantum efficiency of quantum dot based hybrid photonic assemblies. © *2013 AIP Publishing LLC*. [http://dx.doi.org/10.1063/1.4817650]

I. INTRODUCTION

Quantum dots are a class of novel nanoscale materials, which are useful in wide ranging applications from lasers to sensing and photovoltaics.[1–4] The optical properties of isolated quantum dots have been widely studied and reasonably understood in terms of the confinement effect on the electronic band structure.[5] The electrical and optical properties of arrays of quantum dots[6–9] as well as binary assemblies of quantum dots with metal nanoparticles are beginning to be explored.[10–18] Although various applications of such arrays have been envisaged,[9,19–21] the ability to understand and control the optical properties of such arrays depends significantly on understanding of the interactions between the excitons in multiple quantum dots and the plasmons in multiple metal nanoparticles. Most theoretical and experimental works, thus far, have dealt with relatively simple systems involving few or single quantum dot and metal nanoparticles.[11,18]

A key question in all applications of such quantum dot arrays is the conditions of appropriate doping by metal particles so as to enhance the emission leading to more efficient sensors, light emitting or photovoltaic devices, and related aspects. For instance, enormous research has been undertaken to use local optical density of states (LDOS) engineering using photonic crystal devices[22–25] to enhance or quench the emission or radiative decay rates of quantum dots embedded near or inside such devices. Although it is possible to obtain very large quality (Q) factors in such systems, the large mode volumes (V) involved can result in Purcell factors ($F_p = \frac{3\lambda_c^3}{4\pi^2 n^3}\frac{Q}{V}$, λ_c the cavity resonance wavelength and n the refractive index of the medium) that are only moderately high. Also very large Q factors and mode volumes imply both acute specificity of the spectral range of operation and relatively larger size of these devices, which may not be advantageous. Hence recently, Purcell effect mediated decay rate engineering using plasmonic nano-antenna[26–34] or even metallodielectric antenna[35] has been suggested as an alternative with the advantage that although the Q factors are smaller than the corresponding photonic crystal based cavities, huge reduction in mode volumes can be obtained leading to possibility of very high F_p. In addition, such coupling can also be enhanced by reducing the separation between an emitter or quantum dot with a metal nano-antenna. However, eventual F_P will be limited by the fact that non-radiative processes take over for sufficiently small metal particles and separations.[36]

The parameters involved, thus, include the size of the antennae, relative number density, the spatial distribution, and the spectral overlaps (on and off-resonance characteristics). Most studies so far involved control of the decay rates of emitters using a larger size of the antennae and varying the resonance characteristics of the antenna arrays. Here, we show that in the limit, where both the size and the relative number density of the nano-antennae are low (relative volume fractions), especially sensitive control of the radiative and non-radiative decay rates of quantum dots are possible. But such use of the size and distribution in turn needs precise control over local densities of both the antennae and the quantum dots. It has been shown earlier by us and others[15,16,37] that arrays of chemically synthesized Cadmium Selenide (CdSe) quantum dot assemblies doped with gold (Au) nanoparticles can be prepared, based on simple self-assembly methods, using a polymer template, with independent control over their

a)Electronic mail: basu@physics.iisc.ernet.in

respective location, density and size as well as lattice parameters of the arrays. Here, we report new results on photoluminescence (PL) spectroscopy and lifetime measurements on such 2-dimensional (2D) hybrid arrays as a function of increasing number of Au nanoantennae for fixed density of quantum dots. Specifically, extent of overlap between quantum dot PL emission and Au nanoantennae absorption as well as the size of Au nanoparticles determines the PL intensity enhancement/quenching as well as the variation in the PL decay lifetime in such binary arrays. We observe more than 4-fold enhancement of radiative decay rate, Γ_r of the CdSe quantum dots with increasing doping of Au nanoparticles in the case, where the quantum dot PL emission spectra have strong overlap with the surface plasmon resonance (SPR) absorption spectra of the Au nanoantennae[38] (Fig. 3), in a monotonic fashion. Although there is also a concomitant increase in the non-radiative decay rate, Γ_{nr} this increase is only by a factor of $\sim$1.25, leading to large enhancement in the total quantum yield, η. In samples, where the quantum dot emission spectra have less overlap with the SPR absorption spectra[38] (Fig. 4), we observe qualitatively similar trends. However, interestingly we observe that the Γ_{nr} can actually be reduced significantly ($\sim$20%), while the Γ_r still increases although by a maximum of only 1.75 times the pristine sample (L). On the other hand for the samples in which much smaller Au nanoparticles are used to dope the same quantum dot arrays, we find large decrease in Γ_r accompanied by increase in Γ_{nr}, thus leading to strong decrease in η. The cross-over from an increased PL lifetime with low Au nanoantennae doping, to reduced PL lifetime at higher doping for same size and density of quantum dot and Au nanoantennae, points to the interplay of subtle variations of the scattering and absorption contributions of Au nanoparticles to the Purcell factor for decay rates. We have, hence, used discrete dipole approximation (DDA) based numerical modeling, whereby actual dot/particle configurations are considered, which successfully captures the relative non-monotonic behavior of the decay rate variations, although the exact values for some of the samples do not match.

II. METHODS

CdSe quantum dots, with average diameters (D_{CdSe}) of 4 nm and 6 nm and Au nanoparticles (D_{Au}) of mean diameters of 2 nm and 5 nm were synthesized according to methods described elsewhere.[15,16,38] Hybrid arrays of quantum dots and Au nanoparticles were prepared using a polymer template consisting of polystyrene (PS) and polyvinyl pyridine (P4VP) as reported elsewhere.[15,16,38] The dispersion of Au nanoparticles and quantum dots inside the polymer photonic template is schematically shown in Fig. 1. The samples were prepared with different volume fractions of Au nanoparticles, ϕ_{Au}, for a fixed volume fraction, ϕ_{CdSe} (0.054 with respect to the polymer), of CdSe quantum dots (Table I). The extent of ordering of these films can be seen from the respective atomic force microscopy (AFM) images.[38] The average spacing between quantum dot filled P4VP cylinders is found to be $\sim$100 nm, while the nature of dispersion of Au nanoparticles and CdSe quantum dots was similar to that reported earlier.[15,16]

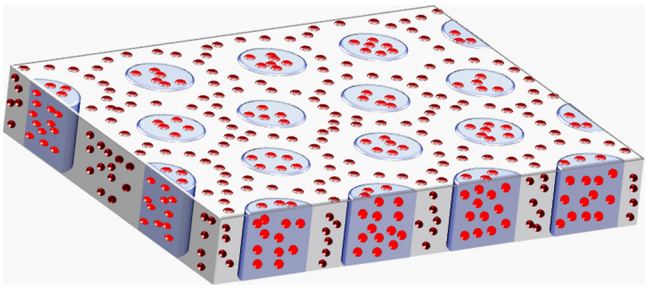

FIG. 1. Schematic representation of hybrid films in the polymer template showing the dispersion of CdSe quantum dots in P4VP block and Au nanoparticles in PS block, indicated by the red and brown dots, respectively.

PL measurements on our samples were performed using a WITec alpha SNOM setup in confocal mode as described earlier.[15,16] The time-resolved PL measurements were performed using a 472 nm laser excitation supplied by the doubled output of a mode-locked Ti:Sapphire laser (Mira 900, Coherent), coupled to a inverted confocal microscope (Nanonics Inc., USA). The data presented here are based on films, in which both the density of quantum dots and Au nanoantenna were varied independently, as shown in Table I.

In order to obtain a microscopic model of the various mechanisms at play leading to such non-trivial variation of decay rates in such partially ordered materials, we have used the DDA model which can accommodate higher spatial complexity as is the case here. Since the most complex and interesting behavior is observed for the larger Au nanoparticle based systems, we have used the DDA model to understand the behavior of the hybrid films based on such films only.

To model the lifetimes measurements of the BCP film studied, we created the lattice of dipoles over a continuous glass surface. The complex polarizability of the lattice elements are calculated from the corresponding refractive indices of materials using lattice-dispersion-relations.[39] We have used the traditional DDA method in conjunction with the Sommerfeld integral relations to compute the Fresnel coefficients and include even the small glass substrate interaction.[40] Dipoles are coupled by the constitutive relations.

TABLE I. Diameter of CdSe quantum dot D_{CdSe}, Au nanoparticles D_{Au}, thickness (t), volume fraction, and number density ratio of CdSe quantum dot to Au nanoparticles for the samples used in the experiments.

Sample Index	D_{CdSe} nm	D_{Au} nm	t nm	ϕ_{Au}/ϕ_{CdSe}	n_{CdSe}/n_{Au}
S	4	…	100	…	…
SL1	4	5	107	0.07	25
SL2	4	5	103	0.21	8.33
SS1	4	2	142	0.07	1.79
SS2	4	2	130	0.21	0.60
L	6	…	100	…	…
LL1	6	5	93	0.07	7.14
LL2	6	5	108	0.21	2.33
LS1	6	2	108	0.07	0.51
LS2	6	2	111	0.21	0.17

$$(\alpha)_i^{-1} P_i = E_{o,i} + \frac{{k_0}^2}{\epsilon_0} \sum_{j \neq i} \bar{G}_{ij} \cdot \bar{P}_j + \sum_{j=1}^{N} \left(\bar{S}_{ij} + \frac{{k_0}^2}{\epsilon_0} \frac{{k_1}^2 - {k_2}^2}{{k_1}^2 + {k_2}^2} G_{ij}^{-1} \right) \cdot P_{ij}, \quad (1)$$

where

$$\bar{G}_{ij} = \left[\bar{I} + \frac{\nabla \nabla}{k^2} \right] (4\pi \parallel \bar{r}_j - \bar{r}_i) \parallel)^{-1} \exp(ik \parallel \bar{r}_j - \bar{r}_i) \parallel)$$

where α_i, $E_{o,i}$, P_i, r_i are the polarizabilty, the electric field in vacuum, the dipole moment of i, and its radius vector, respectively. $\bar{G}_{ij}$ is a 3×3 matrix, so is $\bar{S}_{ij}$ containing Sommerfeld integral terms of the field for dipoles i and j and k_1 and k_2 are the wave numbers for the polymer and the substrate, respectively. The coupled dipole equations are solved using iterative methods like Quasi-Minimal-Residual (QMR) and the steady state polarizations computed. The decay rates/lifetimes of quantum dots are affected by the properties of the surrounding film at the emission wavelength and can be described as a function of their polarization.[41,42] The relative decay rate of any quantum dot in the BCP film (compared to its vacuum rate) for the given volume fraction of Au nanoparticle is

$$\frac{\Gamma}{\Gamma_0} = 1 + \frac{3\Im[\mathbf{E}_r \cdot \mathbf{P}_s]}{2k^3 P_s^2}, \quad (2)$$

where Γ_0 is the decay rate corresponding to vacuum states, Γ, the modified decay rate in presence of Au nanoparticles, $\mathbf{E}_r$, $\mathbf{P}_s$ are the electric field and dipole moment at the quantum dot due to other particles for any volume fraction ϕ_{Au} of the Au nanoparticles. The PL excitation radiation is incident from the top of the film and a plane wave of 488 nm wavelength incident on the film and the corresponding steady state polarizations gives us the absorption cross sections of the quantum dots in the presence of the metal particles (Fig. 2). While previous works have used plane wave approximations only at the PL emission wavelengths as an effective approximation of the change in decay rates,[43] we have observed that Au nanoparticles can alter the absorption by the quantum dots in the film as well (not just PL emission), and hence, this exercise is important.

Further, we computed the effect of point sources emitting at the PL peak wavelength (630 nm and 560 nm for 6 nm and 4 nm quantum dots, respectively) at the location of the quantum dots with the appropriate strengths of the absorption of those quantum dots (these sources represent the emission from the excitons in vacuum). The field scattered back from the other particles on the quantum dot gives us the relative decay rate compared to the quantum dot in vacuum. In the average decay calculations, we make no distinction of the direction of emission and thus assume no coherence in emission of the quantum dots. This point-source model, unlike a plane wave model, ensures that the effect of relative location of the Au nanoparticles with respect to a quantum dot on the emission process is included accurately. The dispersive electric permittivity of quantum dots and nano particles has been extracted from published results.[44,45] The refractive indices of P4VP, PS, and glass have been extracted from well known Sellmeir coefficient fits.

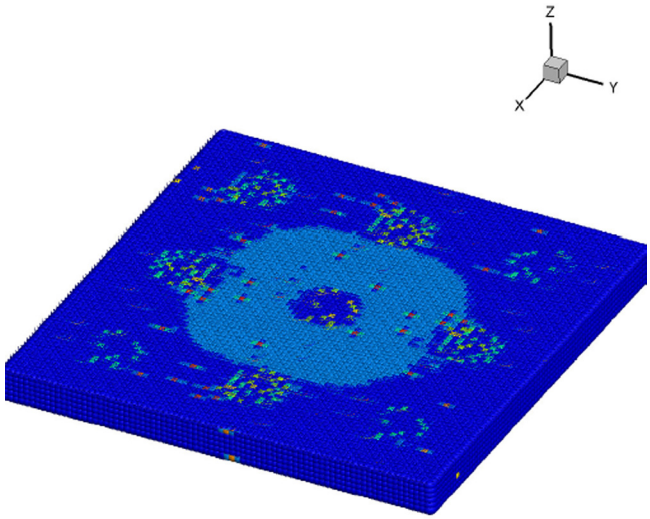

FIG. 2. Representative energy distribution inside the film (energy decreasing from red to blue) due to the plane wave excitation at 488 nm wavelength incident along the normal Z-axis; shown using a Z-section of a 9 cell volume. The Au nanoparticles appear in red primarily, the quantum dots in the inner cylinder appear in yellow or green, and the PS/P4VP matrices are minimally polarized.

III. RESULTS AND DISCUSSION

Figure 3 shows the PL emission spectra from the various hybrid films doped with the larger of the two Au

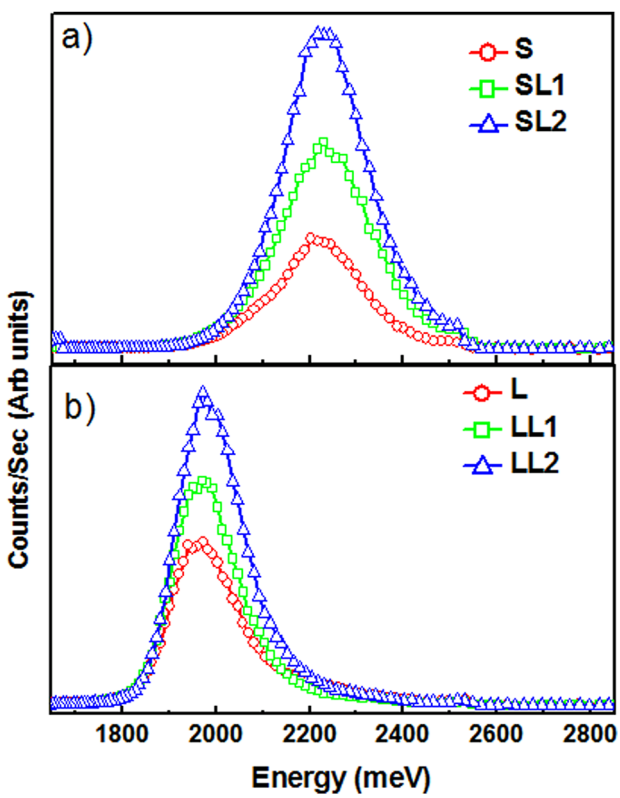

FIG. 3. PL spectra collected from films with small (a) and large (b) quantum dots doped with large metal nano-antennae.

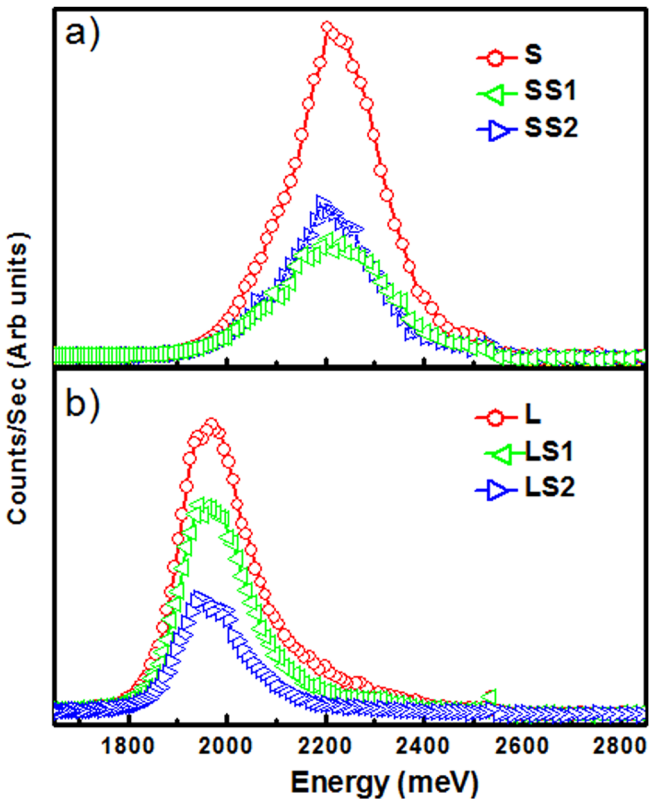

FIG. 4. PL spectra collected from films with small (a) and large (b) quantum dots doped with small metal nano-antennae.

nanoparticle, as indicated in Table I. Incorporation of the larger Au nanoparticles into the quantum dot loaded films (SL1, SL2, LL1, and LL2) leads to enhancement of PL intensity with respect to the undoped films indicating increase in effective η. The enhancement scales with ϕ_{Au}. The effective increase in η is slightly larger for the films with the smaller quantum dots (S-series) as compared to those with the larger quantum dots. It might be noted that the spectral overlap between the PL emission and the SPR absorption is more in the case of the small quantum dots (resonant) as compared to the larger quantum dots (off-resonant).[38] Although the relative volume fraction of CdSe quantum dots and Au nanoparticles is same for both the small and large quantum dot based films, the films with smaller quantum dots have a lower relative number ratio of quantum dots to Au nanoparticles (Table I). So in that sense, the spectral overlap seems to be a relatively strong effect when compared at similar number ratios. In Fig. 4, PL spectra for the films based on the smaller Au nanoparticles. Completely opposite behavior is observed for these hybrid films (SS1, SS2, LS1, and LS2) as compared to those doped with the larger Au nanoparticles. The doping of the films with Au nanoparticles leads to quenching of PL emission, which also scales with ϕ_{Au}. As discussed earlier, this is possibly due to the different dispersion of the Au nanoparticles in the PS matrix. However, it is also possible that the decrease of the relative scattering and absorption contribution with the reduction of Au nanoparticle size leads to the observed quenching.

To obtain further insight into the Au nano-antenna size and spectral overlap dependence on the efficiency of the PL decay rate engineering, especially the relative contribution of the Purcell factor modified radiative and non-radiative decay rates, we studied the nature of the decay of PL emission from the films. Figure 5 shows results of several PL lifetime measurements on the same films doped with larger Au nanoparticles, for which we discussed the PL spectra above. For simplicity, we fitted all decay curves with a single exponential function and the results are shown in Table I. Details of the results of fitting the lifetime data with more complicated functions are provided in Ref. 38 (Table I). The qualitative trends of the observed variations of the extracted time constants are very similar for both analyses. Interestingly, while the lifetime changes monotonically for the resonant case (SL series), we find strong non-monotonic variation of the lifetime for the off-resonant case (LL series). The extracted values of PL decay time and calculated values of Γ_r and Γ_{nr} for the CdSe quantum dots in the hybrid films are listed in Table II and described in Ref. 38. For the resonant samples, we observe more than four fold increase in the Γ_r, while the Γ_{nr} also increases, for the same ϕ_{Au}, albeit by a factor of 1.25 only. This leads to the significant increase in effective η of the resonant case samples. Similarly, Fig. 6 displays the lifetime data for the hybrid films doped with the smaller Au nanoparticles. The trends are similar to those of the data from the films based on the larger Au nanoparticles. Remarkably, though, in the off-resonant case we are able to observe reduction in Γ_{nr}, while the Γ_r still shows slight increase. From the obtained values of Γ_r and Γ_{nr}, we also conclude that the measured non-monotonic variation in PL lifetime decay in L-series (off-resonant) samples is largely due to the variation of Γ_{nr} with ϕ_{Au}.

Calculations using DDA were performed only for the cases, where the dimensions of Au nanoparticles and quantum dots are similar (SL1, SL2, LL1, LL2), as mentioned

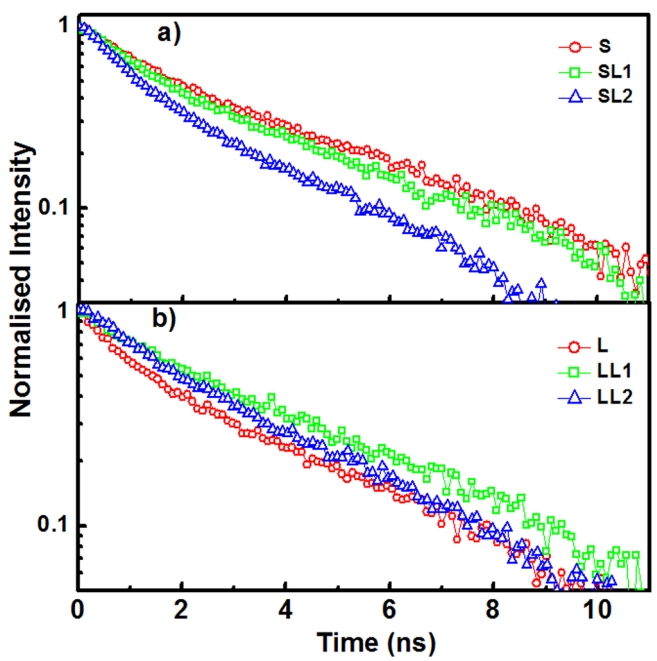

FIG. 5. PL decay curve from films doped with large Au nano-antennae with small quantum dots (a) S (○), SL1 (□), SL2 (△), and (b) large quantum dots L (○), LL1 (□), LL2 (△).

TABLE II. Extracted values of experimental (τ), normalized lifetimes in comparison to the respective quantum dot films (τ/t_{ref}), calculated values using DDA method (τ/t_{ref}), the values of quantum yield, η and the calculated values of radiative and non radiative decay rates for the samples used in the experiments.

Sample Index	τ (ns)	τ/t_{ref} (Exp.)	τ/t_{ref} (Calc.)	η	Γ_r ns^{-1}	Γ_{nr} ns^{-1}
S	4.25 ± 0.01	1.00	1.00	0.05	0.011	0.224
SL1	3.18 ± 0.02	0.75	0.982	0.10	0.030	0.285
SL2	3.05 ± 0.03	0.72	0.894	0.14	0.047	0.281
SS1	4.23 ± 0.02	0.99	…	0.02	0.005	0.232
SS2	3.90 ± 0.02	0.92	…	0.02	0.006	0.251
L	3.92 ± 0.02	1.00	1.00	0.07	0.018	0.237
LL1	4.87 ± 0.01	1.24	1.004	0.08	0.017	0.193
LL2	3.87 ± 0.04	0.98	0.97	0.12	0.031	0.228
LS1	4.48 ± 0.02	1.14	…	0.05	0.011	0.213
LS2	3.86 ± 0.01	0.98	…	0.02	0.006	0.253

earlier, so as to allow for an effective lattice representation of volume fractions of both particles. The average relative change in lifetimes of quantum dots due to the addition of the Au nanoparticles is tabulated in Table II. Since the vacuum rates are not measured, we normalize the results by the case of quantum dots in the matrix without any Au nanoparticles. The relative trends of variation of the normalised decay rates with ϕ_{Au}, are similar to the experimental data. It is indeed observed from these results that the lifetimes of the quantum dots can increase even as the PL emission enhancement occurs; while the field-enhancement in this case increases PL emission without affecting the lifetime, a small Purcell inhibition of the radiative process does result in a slower decay. Thus, the observed non-monotonic variation of the normalised decay rates are qualitatively matched by the DDA calculations. However, the small quantitative mis-match could be due to the presence of cooperative interaction between quantum dots mediated by the plasmons on the Au nanoparticles.[46] In addition to the spectral characteristics of the mechanisms discussed above, their relative combination and the net effect is modulated by the spatial distribution and number density of the Au nanoparticles around the quantum dots. Some of this later aspect is captured well by the DDA based simulations.

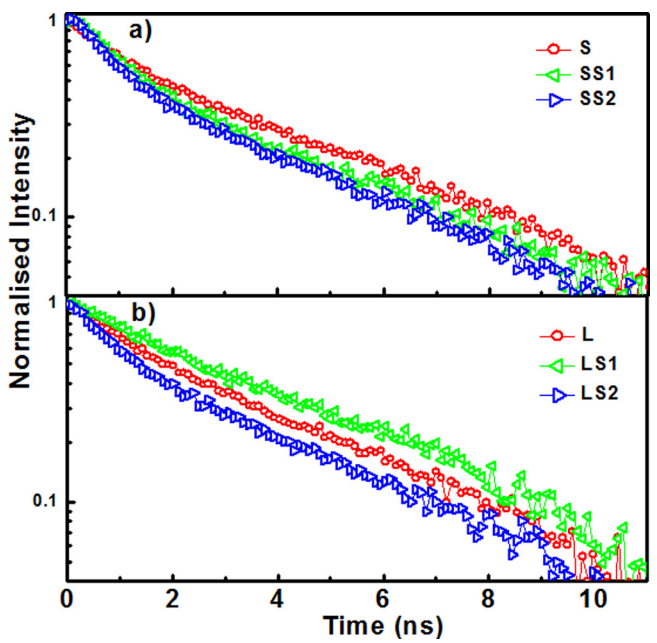

FIG. 6. PL decay curve from films embedded with small Au nano-antennae and small quantum dots, (a) S (○), SS1 (◁), SS2(▷), and with large quantum dots (b) L (○), LS1 (◁), LS2 (▷).

IV. CONCLUSIONS

In conclusion, we have presented experimental observations of photoluminescence intensity and decay lifetimes of CdSe quantum dot arrays doped with Au nanoparticles, acting as simple nano-antenna, along with relevant analytical and computational results. We observe both enhancement and quenching of PL intensity of quantum dot arrays due to added Au nanoparticles, with respect to undoped quantum dot arrays. The corresponding variation in lifetime of PL spectra decay shows a hitherto unobserved, non-monotonic variation with Au nanoparticle doping. We have shown that plasmonic Purcell effect is quite effective for the 5 nm Au nano-antenna leading to more than four times increase in radiative rate at spectral resonance, for the highest doping concentration of Au nanoantennae, and only ~1.75 times enhancement when the quantum dot PL and Au nanoantennae SPR are spectrally detuned. Significantly, for spectral off-resonance samples, we could engineer reduction of Γ_{nr} along with increase of Γ_r. We have demonstrated that the relevance of our work goes beyond the particular material that we have used in our experiments and, in principle, applicable towards understanding of optical properties of a wide variety of multi- functional assemblies of quantum dots and metal nanoparticles. Future work would aim at studying more specifically, through careful experiments, the regime of possible breakdown of the superposition of independent optical excitations in a multi-particle-emitter scenario, as well as to try to incorporate cooperative optical interactions in our theoretical model, both analytically and numerically.

ACKNOWLEDGMENTS

We acknowledge that the use of the Center for Nanoscale Materials was supported by the US. Department of Energy, Office of Science, Office of Basic Energy Sciences under Contract No. DE-AC02-06CH11357. We acknowledge the assistance of David Gosztola and Gary Wiederrecht, both of CNM for lifetime measurements and useful discussions. We acknowledge DST-IISc nano science for TEM and optical measurements. M.H. acknowledges UGC for financial support.

[1]S. Fafard, K. Hinzer, S. Raymond, M. Dion, J. McCaffrey, Y. Feng, and S. Charbonneau, Science **274**, 1350 (1996).
[2]J. Hendrickson, B. C. Richards, J. Sweet, S. Mosor, C. Christenson, D. Lam, G. Khitrova, H. M. Gibbs, T. Yoshie, A. Scherer, O. B. Shchekin, and D. G. Deppe, Phys. Rev. B **72**, 193303 (2005).
[3]I. L. Medintz, H. T. Uyeda, E. R. Goldman, and H. Mattoussi, Nature Mater. **4**, 435 (2005).
[4]J. Tang and E. H. Sargent, Adv. Mater. **23**, 12 (2011).
[5]A. D. Yoffe, Adv. Phys. **51**, 799 (2002).

[6]C. R. Kagan, C. B. Murray, M. Nirmal, and M. G. Bawendi, Phys. Rev. Lett. **76**, 1517 (1996).
[7]E. V. Shevchenko, D. V. Talapin, N. A. Kotov, S. ÓBrien, and C. B. Murray, Nature **439**, 55 (2006).
[8]D. V. Talapin and C. B. Murray, Science **310**, 86 (2005).
[9]A. J. Nozik, M. C. Beard, J. M. Luther, M. Law, R. J. Ellingson, and J. C. Johnson, Chem. Rev. **110**, 6873 (2010).
[10]Z. Jacob, I. I. Smolyaninov, and E. E. Narimanov, Appl. Phys. Lett. **100**, 181105 (2012).
[11]A. O. Govorov, G. W. Bryant, W. Zhang, T. Skeini, J. Lee, N. A. Kotov, J. M. Slocik, and R. R. Naik, Nano Lett. **6**, 984 (2006).
[12]M. Haridas, L. N. Tripathi, and J. K. Basu, Appl. Phys. Lett. **98**, 063305 (2011).
[13]J. S. Biteen, D. Pacifici, N. S. Lewis, and H. A. Atwater, Nano Lett. **5**, 1768 (2005).
[14]R. J. Walters, R. V. A. van Loon, I. Brunets, J. Schmitz, and A. Polman, Nature Mater. **9**, 21 (2010).
[15]M. Haridas, J. K. Basu, D. J. Gosztola, and G. P. Wiederrecht, Appl. Phys. Lett. **97**, 083307 (2010).
[16]M. Haridas and J. K. Basu, Nanotechnology **21**, 415202 (2010).
[17]H. Noh, Y. Chong, A. D. Stone, and H. Cao, Phys. Rev. Lett. **108**, 186805 (2012).
[18]V. N. Pustovit and T. V. Shahbazyan, Phys. Rev. Lett. **102**, 077401 (2009).
[19]D. J. Bergman and M. I. Stockman, Phys. Rev. Lett. **90**, 27402 (2003).
[20]V. I. Klimov, A. A. Mikhailovsky, S. Xu, A. Malko, J. A. Hollingsworth, C. A. Leatherdale, H. J. Eisler, and M. G. Bawendi, Science **290**, 314 (2000).
[21]M. A. Noginov, G. Zhu, A. M. Belgrave, R. Bakker, V. M. Shalaev, E. E. Narimanov, S. Stout, E. Herz, T. Suteewong, and U. Wiesner, Nature **460**, 1110 (2009).
[22]K. Hennessy, A. Badolato, M. Winger, D. Gerace, M. Atatüre, S. Gulde, S. Fält, E. L. Hu, and A. Imamoğlu, Nature **445**, 896 (2007).
[23]H. Iwase, D. Englund, and J. Vucković, Opt. Express **18**, 16546 (2010).
[24]T. Lund-Hansen, S. Stobbe, B. Julsgaard, H. Thyrrestrup, T. Sünner, M. Kamp, A. Forchel, and P. Lodahl, Phys. Rev. Lett. **101**, 113903 (2008).
[25]D. Englund, D. Fattal, E. Waks, G. Solomon, B. Zhang, T. Nakaoka, Y. Arakawa, Y. Yamamoto, and J. Vucković, Phys. Rev. Lett. **95**, 013904 (2005).
[26]L. Novotny and N. Van Hulst, Nature Photon. **5**, 83 (2011).
[27]S. Kühn, U. Hakanson, L. Rogobete, and V. Sandoghdar, Phys. Rev. Lett. **97**, 017402 (2006).
[28]T. V. Teperik and A. Degiron, Phys. Rev. Lett. **108**, 147401 (2012).
[29]V. Giannini, A. I. Fernández-Domínguez, S. C. Heck, and S. A. Maier, Chem. Rev. **111**, 3888 (2011).
[30]M. Venkatapathi, J. Quant. Spectrosc. Radiat. Transf. **113**, 1705 (2012).
[31]H. Mertens, A. F. Koenderink, and A. Polman, Phys. Rev. B **76**, 115123 (2007).
[32]C. Vandenbem, D. Brayer, L. S. Froufe-Pérez, and R. Carminati, Phys. Rev. B **81**, 085444 (2010).
[33]J. N. Farahani, D. W. Pohl, H. J. Eisler, and B. Hecht, Phys. Rev. Lett. **95**, 017402 (2005).
[34]O. L. Muskens, V. Giannini, J. A. Sánchez-Gil, and J. G. Rivas, Nano Lett. **7**, 2871 (2007).
[35]X. Chen, M. Agio, and V. Sandoghdar, Phys. Rev. Lett. **108**, 233001 (2012).
[36]R. Carminati, J. J. Greffet, C. Henkel, and J. M. Vigoureux, Opt. Commun. **261**, 368 (2006).
[37]Y. Lin, A. Boker, J. He, K. Sill, H. Xiang, C. Abetz, X. Li, J. Wang, T. Emrick, S. Long, Q. Wang, A. Balazs, and T. P. Russell, Nature **434**, 55 (2005).
[38]See supplementary material at http://dx.doi.org/10.1063/1.4817650 for Uv-Vis absorption spectra and TEM images of CdSe quantum dots and Au nanoparticles, preparation of the hybrid films, AFM images for the quantum dot film and hybrid film.
[39]B. T. Draine and J. Goodman, Astrophys. J. **405**, 685 (1993).
[40]R. Schmehl, B. M. Nebeker, and E. D. Hirleman, J. Opt. Soc. Am. A **14**, 3026 (1997).
[41]I. Prigogine, S. A. Rice, R. R. Chance, A. Prock, and R. Silbey, Adv. Chem. Phys. **37**, 65 (1978).
[42]V. V. Klimov and M. Ducloy, Phys. Rev. A **69**, 013812 (2004).
[43]J. S. Biteen, L. A. Sweatlock, H. Mertens, N. S. Lewis, A. Polman, and H. A. Atwater, J. Phys. Chem. C **111**, 13372 (2007).
[44]M. Alves-Santos, R. D. Felice, and G. Goldoni, J. Phys. Chem. C **114**, 3776 (2010).
[45]P. B. Johnson and R. W. Christy, Phys. Rev. B **6**, 4370 (1972).
[46]M. Haridas, J. K. Basu, A. K. Tiwari, and M. Venkatapathi, "Collective modes of emission in multi-particle Quantum dot-metal hybrid films" (to be published).